


ORIGINAL ARTICLE

The *RRAS2* pathogenic variant (c.67G>T; p. Gly23Cys) produces Noonan syndrome with embryonal rhabdomyosarcoma

Lan Zeng¹ | Jin Wang¹ | Hui Zhu² | Yu Huang² | Yi Deng¹ | Ping Wei¹ | Jing Nie³ | Bei Tang⁴ | Ai Chen² | Shuyao Zhu² 

¹Department of Medical Genetics and Prenatal Diagnosis, Sichuan Provincial Maternity and Child Health Care Hospital, Chengdu, China

²Department of Pediatrics, Sichuan Provincial Maternity and Child Health Care Hospital, Chengdu, China

³Department of Children's Health Care, Sichuan Provincial Maternity and Child Health Care Hospital, Chengdu, China

⁴Department of Ultrasound, Sichuan Provincial Maternity and Child Health Care Hospital, Chengdu, China

Correspondence

Shuyao Zhu, Department of Pediatrics, Sichuan Provincial Maternity and Child Health Care Hospital, Chengdu 610031, China.

Email: 330986673@qq.com

Funding information

Chengdu Bureau of Science and Technology Project, Grant/Award Number: 2021-YF05-01658-SN

Abstract

Background: Noonan syndrome (NS) due to the *RRAS2* gene, the pathogenic variant is an extremely rare RASopathies. Our objective was to identify the potential site of *RRAS2*, combined with the literature review, to find the correlation between clinical phenotype and genotype. De novo missense mutations affect different aspects of the *RRAS2* function, leading to hyperactivation of the RAS-MAPK signaling cascade.

Methods: Conventional G-banding was used to analyze the chromosome karyotype of the patient. Copy number variation sequencing (CNV-seq) was used to detect the chromosomal gene microstructure of the patient and her parents. The exomes of the patient and her parents were sequenced using trio-based whole exome sequencing (trio-WES) technology. The candidate variant was verified by Sanger sequencing. The pathogenicity of the variant was predicted with a variety of bioinformatics tools.

Results: Chromosome analysis of the proband revealed 46, XX, and no abnormality was found by CNV-seq. After sequencing and bioinformatics filtering, the variant of *RRAS2*(c.67G>T; p. Gly23Cys) was found in the proband, while the mutation was absent in her parents. To the best of our knowledge, our patient was with the typical Noonan syndrome, such as short stature, facial dysmorphism, and developmental delay. Furthermore, our study is the first case of NS with embryonal rhabdomyosarcoma (ERMS) caused by the *RRAS2* gene mutation reported in China.

Conclusions: Our investigations suggested that the heterozygous missense of *RRAS2* may be a potential causal variant in a rare cause of Noonan syndrome, expanding our understanding of the causally relevant mutations for this disorder.

KEYWORDS

Noonan syndrome, RASopathy, *RRAS2*, whole exome sequencing

This is an open access article under the terms of the [Creative Commons Attribution-NonCommercial-NoDerivs](https://creativecommons.org/licenses/by-nc-nd/4.0/) License, which permits use and distribution in any medium, provided the original work is properly cited, the use is non-commercial and no modifications or adaptations are made.

© 2023 The Authors. *Molecular Genetics & Genomic Medicine* published by Wiley Periodicals LLC.

1 | INTRODUCTION

Noonan syndrome (NS [MIM: 163950]) is an autosomal dominant or recessive disorder, characterized by short stature, variable developmental delay, distinctive facial features, and congenital cardiac defects, as well as variable neurocognitive impairment and predisposition to malignancies (Roberts et al., 2013; Tartaglia et al., 2011; Yu et al., 2023). Approximately 80% of NS-positive individuals have mutations in genes whose products are involved in the RAS/mitogen-activating protein kinase (MAPK) pathway. The MAPK pathway and as such NS belong to a group of diseases collectively termed RASopathies (Tidyman & Rauen, 2009). NS is the most common disease in RASopathies, with a neonatal prevalence of 1/2000~1/1000, and is genetically heterogeneous and mutations in more than ten genes have been reported to be the basis of this disease. Some genes related to the RAS-MAPK pathway have been implicated in NS, including the *PTPN11*, *SOS1*, *SOS2*, *RAF1*, *RIT1*, *KRAS*, *NRAS*, *MRAS*, *BRAF*, *MAP2K1*, and *LZTR1* genes (Yamamoto et al., 2015). Among RAS GTPases, *RRAS2* showed the highest amino acid identities with *HRAS*, *KRAS*, and *NRAS*. A series of studies have reported that *RRAS2* (RAS related 2, also known as TC21, teratocarcinoma 21) (MIM: 600098) is a member of the RAS superfamily of GTPases and pathogenic variants of *RRAS2* can also cause NS (Capri et al., 2019; Niihori et al., 2019).

Somatic mutations in *RRAS2* have been shown to contribute to tumorigenesis (Nakhaei-Rad et al., 2018). *RRAS2* controls multiple cellular processes, including proliferation, survival, and migration, and its functional dysregulation has been documented to contribute to oncogenesis (Erdogan et al., 2007; Graham et al., 1999). Most subjects with pathogenic variants of *RRAS2* showed classic features of NS, including characteristic facial features, short stature, wide interocular distance, wide intermammary distance, and congenital deafness. In particular, variant p.Q72L *RRAS2* presents with more pronounced facial dysmorphism, macrocephaly, non-obstructive hydrocephalus, and severe neurological manifestations, remained critically ill from birth, and died at very young ages. Here, we report a case of NS patient with rhabdomyosarcoma, which was found to be a novel heterozygous variant in the *RRAS2* gene by WES.

However, the exact molecular mechanism of Noonan syndrome due to *RRAS2* remains unclear. To study the genetic basis of the disease, we performed whole exome sequencing of the patient and the peripheral blood of her parents.

2 | MATERIALS AND METHODS

2.1 | Ethical compliance

The study was approved by the Institutional Ethics Committee of the Sichuan Provincial Hospital for Women and Children (protocol code: 20230331-027 and date:2023.03. 31).

2.2 | Sample collection

The blood samples from the proband and her parents were collected and kept at -80°C .

2.3 | Chromosome karyotype analysis and copy number variation sequencing

Karyotyping was performed according to the International System for Human Cytogenetic Nomenclature (ISCN2020) standard, using a fully automated scanning system (ZEISS, Germany). Genomic DNA (10ng) was fragmented and the DNA library was constructed as previously described, with low-depth high-throughput sequencing (Chigene Medical Laboratory, Beijing, China). The pedigree of the whole genome was tested and the sequencing data were compared to the hg19 reference genome. Chromosomal aneuploidy variation and CNV above 100kb were recorded and analyzed.

2.4 | Exome sequencing and Sanger sequencing

Genomic DNA was isolated from peripheral blood leukocytes using the QIAamp DNA Blood Mini Kit (Dusseldorf, Germany) according to the manufacturer's instructions. DNA content and quality were determined using nanodrop and agarose gelelectrophoresis, respectively. Genomic DNA was broken into random fragments and purified. The exomes of the patient and her parents were sequenced using family trio-WES technology. Genome-wide exons were captured using IDT The xGen Exome Research Panel v2.0 whole-exon capture chip. After enrichment with quality control, the captured fragments were used for genomic library preparation and sequenced on the applied Biosystems 3730xl DNA Analyzer. The average sequencing depth is 100 \times and more than 98% of the area reached more than 30 \times of the coverage. To validate the candidate

pathogenic mutations in the patient and her parents, Sanger sequencing was performed using the ABI 3730xl sequencer (Applied Biosystems company).

2.5 | High-sensitivity sequencing analysis of mitochondrial DNA

Using the Illumina NovaSeq 6000 sequencing platform, high-throughput mitochondrial DNA sequencing of the patient was performed, and the sequencing data were aligned with the mitochondrial genome reference sequence.

2.6 | In silico analysis

We used whole-exome sequencing and in-depth mutation analysis to find the potential causes. Then, Picard v1.134 (<http://broadinstitute.github.io/picard/>) was used to mark duplicate reads. Variants were called by Genome AnalysisTK (GATK v3.7) and annotated by ANNOVAR. Genetic variant filtering includes removing variants with frequencies $\geq 5\%$ in the GnomAD, ESP, 1000Genomes databases, and local normal human databases, and removing non-functional genetic variants (e.g., sense variants, non-coding region variants, etc.). SIFT (<http://sift.jcvi.org/>), REVEL, PolyPhen2 (<http://genetics.bwh.harvard.edu/pph2/>), and MutationTaster (<http://www.mutationtaster.org/>) software were used to predict the effect of variants on protein structure and function. Clinical symptoms were compared, referring to OMIM, HGMD, ClinVar, MITOMAP, PubMed, and other databases and literature, and candidate gene variants were verified in families. The identified sequence variant was further interpreted and classified according to the American College of Medical Genetics and Genomics (ACMG) guidelines.

3 | RESULTS

3.1 | Clinical report

The patient is a currently 9-year and 2-month-old female, who was born at 38 weeks gestation by vaginal delivery; she was born to a noconsanguineous healthy family. A prenatal ultrasound at 28 weeks of gestation demonstrated “fetal cerebral ventriculomegaly” fetal hydrocephalus was detected by prenatal magnetic resonance imaging (MRI). At birth, her head circumference was 36 cm (>97 th percentile), weight was 3.4 kg (75th to 90th percentile), and height was 46 cm (5th percentile). At 3 months of age, the

parents noticed that the baby would not raise her head, had enlarged anterior fontanelle (5 cm \times 5 cm), and was hypotonic. A medical evaluation found unilateral hearing loss and total developmental delays in the baby. Brain MRI revealed hydrocephalus and possible brain dysplasia. She had delayed motor and language development. At the age of two, she learnt to stand and pronounce simple words. At 2 years and 5 months old, she was found with a distended abdomen. Two-dimensional ultrasound demonstrated that inhomogeneous low echo structure. The tumor was surgically removed, which was pathologically diagnosed as abdominal embryonal rhabdomyosarcoma (ERMS) and followed by chemotherapy. Tumor pathology immunohistochemical examination showed that positive expression of CD56, INI-1, Myogenin, Desmin, and positive rate of Ki-67 was 45%, while ALK, CD117, CD34, CD68, CD99, CK, EMA, SMA, S-100, and SYN were negative expression and consistent with ERMS in combination with immunohistochemistry. At 3 years and 11 months of age, abdominal PET-CT detected a recurrence of the tumor. The tumor was treated with radiation therapy for 1 year. At 4 years 9 months of age, the patient had vomiting due to intestinal adhesion and had partial bowel resection. There was no tumor recurrence after 5 years of observation. The delay in global development became more pronounced when she started elementary school and she had difficulty in arithmetic and writing skills. The patient was presented to our pediatric neurology department. Physical examination revealed a head circumference of 54.5 cm (normal), a weight of 18 kg (<1 st percentile), and a height of 114 cm (<1 st percentile). The patient also exhibits dysmorphic features prominent forehead, high hairline, thinning forehead hair, wide eye spacing, nasal bridge collapse, high palatal arch, and widened bilateral papilla spacing. She had no scoliosis but had cryptomerorachischisis, no cardiac malformation, and no cardiomyopathy. She was tested on the Mini-mental State Examination (MMSE) and scored 0 on one of the items, ‘100 consecutive minus 7’. Her gross motor and language development was within normal range, and her Intelligence Quotient (IQ) test value was 63 (mild intellectual disability; [Figure 1](#)).

3.2 | Genetic and bioinformatics analysis

In this study, karyotype results of the patient showed 46, XX, which no clinically clear pathogenic variants of CNV were found, and no variant sites with high mitochondrial DNA pathogenic levels were detected. In this study, the patient was found to be a heterozygous missense mutation of *RRAS2* (c.67G>T; p. Gly23Cys). However, the mutation was not detected at this locus in either parent, suggesting that the mutation was a

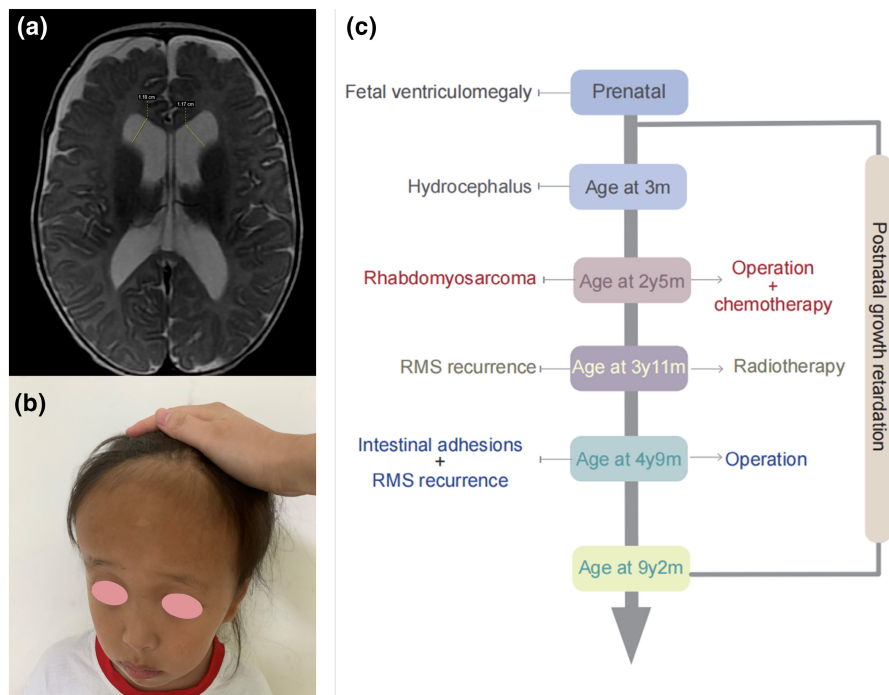


FIGURE 1 (a) MRI brain (index patient): Axial sections showing hydrocephalus. (b) Clinical photographs showing dysmorphic features of the index. (c) Clinical manifestations and the timeline of the index.

new variant (PS2). This mutation is located in the hot-spots (PM1). The heterozygous de novo mutation was consistent with the pathogenesis of autosomal dominant inheritance (AD) disease, and the co-segregation of phenotypes and genotypes of the patient and family members was also consistent. So far, this mutation had not been reported in gnomAD, 1000 Genomes Project, and SNP database (PM2). The ClinVar database included the same sites but different amino acid changes, and it has been reported that Noonan syndrome 12 type (PM5). Furthermore, deleterious mutations by various protein software such as SIFT, Polyphen2, and Mutation Taster (PP3). According to the guide—ACMG, the evidence of a PS2, a PM1, a PM2, a PM5, and a PP3, indicates that the mutation was harmful and destructive to protein function. According to the ACMG guidelines, we classified c.67G>T as pathogenic. By genetic testing, except for *RRAS2*, we found that two other genetic variants (*CDH23/MAN2B1*) were clinically insignificant variants according to ACMG pathogenic ratings, and autosomal recessive disorders with single heterozygous carriers. Therefore, it is considered that other gene variations do not have clinical diagnostic significance for the disease.

3.3 | Sanger sequencing

To further validate heterozygous missense variants of c.67G>T mutation in *RRAS2*, Sanger sequencing was performed. The results showed that the patient found the mutation of *RRAS2* c.67G>T. However, the mutation was

not found in her parents. The Sanger validation result was consistent with the WES analysis.

4 | DISCUSSION

Noonan syndrome (NS) is a relatively common cause of dwarfism, heart malformations, and mental retardation of neurodevelopmental disorders, and more subtypes have been found. Tetsuya Niihori and Yline Capri discovered a new Noonan syndrome gene, *RRAS2*, almost simultaneously in 2019. NS caused by the *RRAS2* gene is called NS 12 type. Over-activation of the RAS-MAP kinase molecular signaling pathway is the pathogenesis of NS (Salem et al., 2016).

Missense mutations in highly conserved amino acid residues of *RRAS2* affect different aspects of *RRAS2* function, including nucleotide binding, GTP hydrolysis, and binding with effectors, leading to hyperactivation of the MAPK signaling cascade. NS-causing variants of *RRAS2* affect highly conserved residues, and the corresponding amino acids, including two mutational hotspot areas of RAS proteins (Gly22-to-Gly26, Ala70, and Gln72) (Figure 2).

Among the 15 reported patients (Table 1), twelve had missense variants and three had fragment duplication variants. Based on the literature search, the reported *RRAS2* variants include c.215A>T(p. Gln72Leu), c.212G>A(p. Gly71Glu), c.208G>A(p. Ala70Thr), c.[216A>T;224T>G] (p.[(Gln72His); (Phe75Cys)]), c.70_78dup(p. Gly24_Gly26dup), c.65_73dup(p. Gly22_Gly24dup), c.68G>T(p. Gly23Val), c.67G>T(p. Gly23Cys).

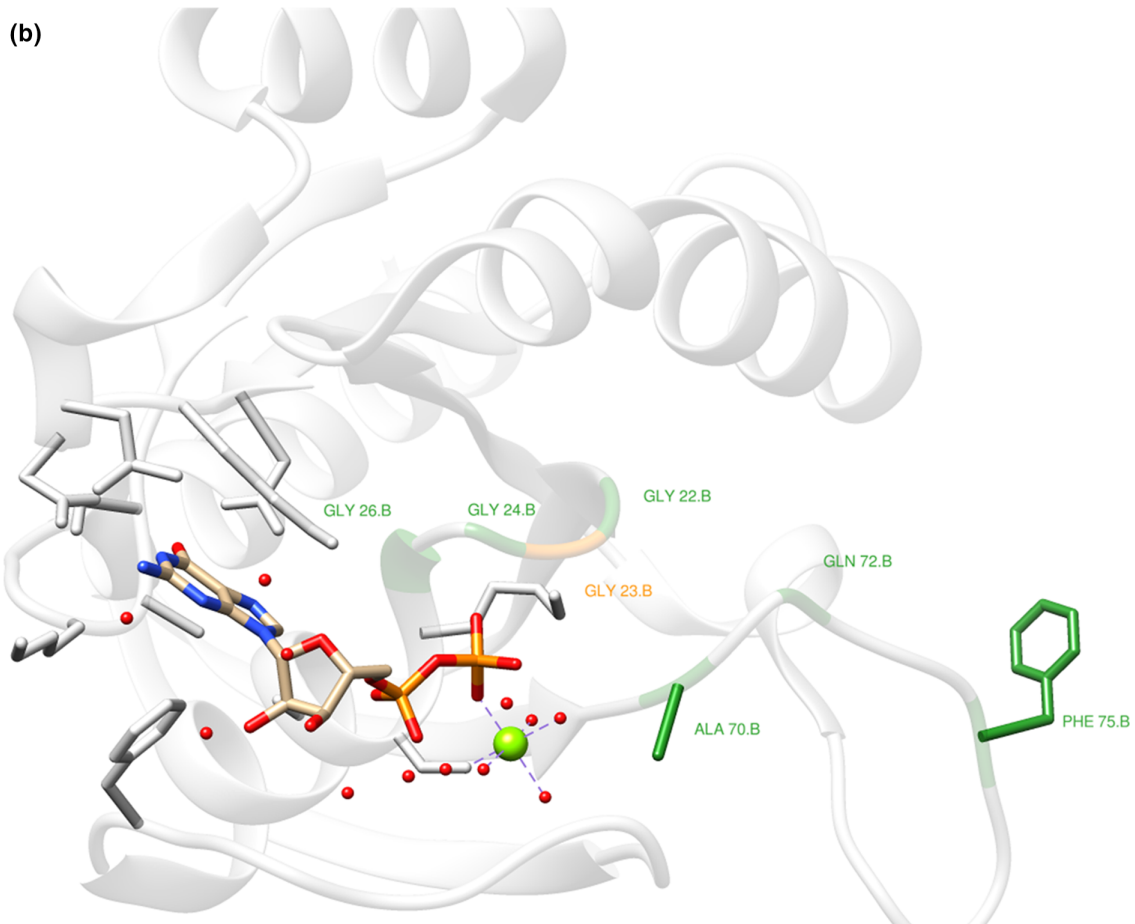
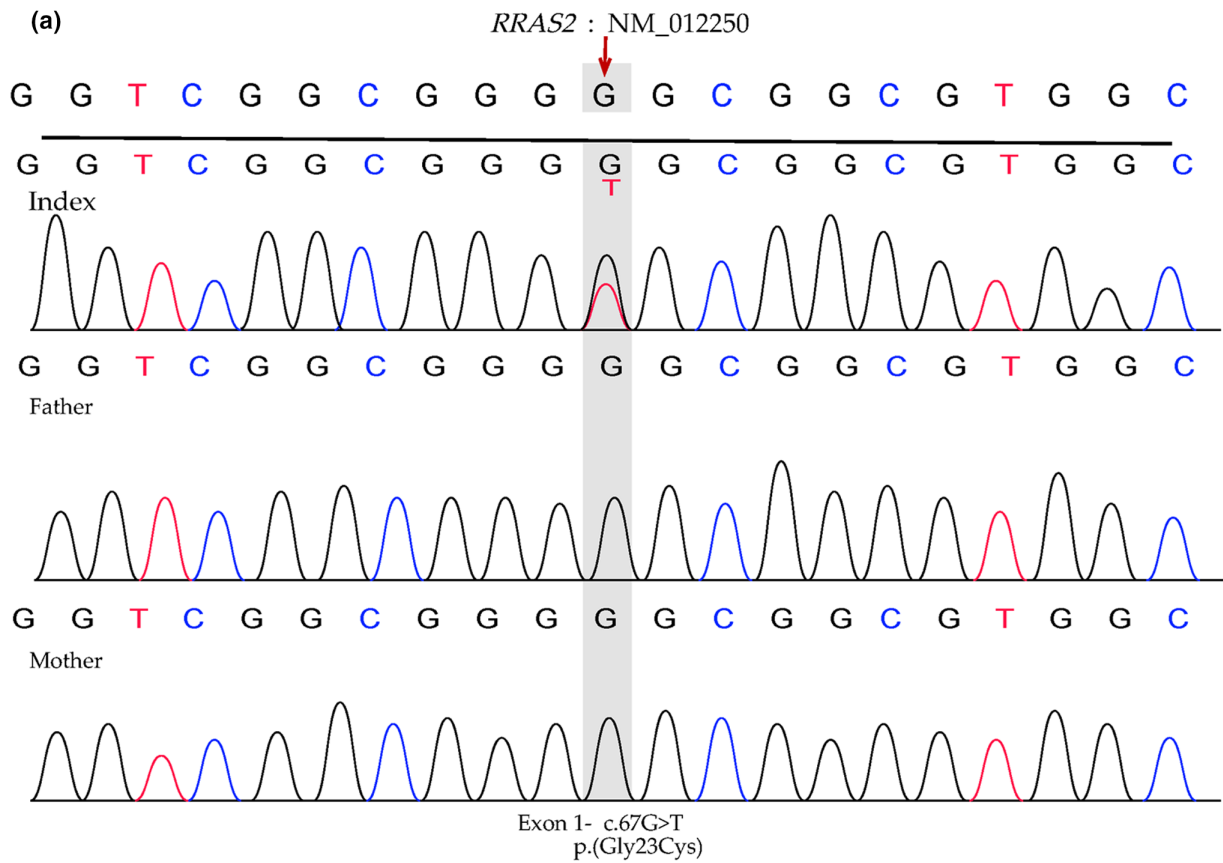


FIGURE 2 (a) Sanger sequencing chromatograms of *RRAS2* index's family. (b) The 3D structure of *RRAS2* protein, and genotype of 15 Patients with heterozygous *RRAS2* variants.

TABLE 1 Noonan Syndrome in Individuals with *RRAS2* Mutations and molecular characterization.

	Patient 1	Patient 2	Patient 3	Patient 4	Patient 5	Patient 6	Patient 7
<i>RRAS2</i> variants	c.[216A>T; 224T>G]	c.215A>T	c.215A>T	c.215A>T	c.212G>A	c.208G>A	c.208G>A
Predicted protein effect	p.[(Gln72His); (Phe75Cys)]	p. Gln72Leu	p. Gln72Leu	p. Gln72Leu	p. Gly71Glu	p. Ala70Thr	p. Ala70Thr
Gender	F	M	M	M	M	F	F
Prenatal features	NA	NA	Cardiac abnormalities	Polyhydramnios	Placenta previa	NA	NA
Age at evaluation	4 years	3 years	2 week	2 week	8 month	32 years	40 years
Height	(−2.4 SD)	(−5.9 SD)	NA	(+1.0 SD)	66.7 cm (−2SD)	(−1.3 SD)	(+1.3 SD)
Weight	NA	NA	NA	3.31 kg (+0.9 SD)	9.5 kg (0SD)	NA	59 kg (+0.1 SD)
Head circumference	NA	NA	NA	36.5 cm (+2.1 SD)	44 cm (0SD)	52.5 cm (−2.2 SD)	55.5 cm (+0.2 SD)
Facial anomalies	Typical	Suggestive	Multiple anomalies	Typical	Suggestive	Suggestive	Mild
Intellectual disability (ID)	Mild	Severe	NA	NA	Moderate global delay		
Neurology	Macrocephaly, enlarged ventricles		Hydrocephalus	Dandy-Walker variant	Delayed myelin development	–	–
Hearing loss	NA	NA	NA	NA	+	NA	NA
Eye abnormalities	NA	NA	NA	Iris and chorioretinal colobomas	–	–	Strabismus
Heart abnormalities	–	DCM	TOF	Suspected fetal arrhythmia	PFO	VSD	–
Malignancy	–	–	–	Myeloproliferative disorder	–	–	–
Other features	Pectus excavatum	Pectus excavatum/ cryptorchidism	Hypoplastic scrotum	Cryptorchidism	–	–	–
References	Niihori et al. (2019)	Niihori et al. (2019)	Capri et al. (2019)	Weinstock and Sadler (2022)	Yu et al. (2023)	Capri et al. (2019)	Capri et al. (2019)

Note: P15 This case was from the Department of Pediatrics, Sichuan Provincial Maternity and Child Health Care Hospital.

Abbreviations: DCM, dilated cardiomyopathy; F, female; NA, not applicable; PFO, patent foramen ovalet; SD, standard deviation; TOF, tetralogy of Fallot; VSD, ventricular septal defect.

Specifically, the amino acid stretch that encompasses Gly22 to Gly26 constitutes part of the phosphate binding loop that is responsible for binding to the phosphate groups of either GTP or GDP. Residues play a critical role in nucleotide binding and hydrolysis by contacting the b-g phosphate of GTP, making part of the phosphate-binding loop constituted by the amino acid stretch that includes Gly22-to-Gly26 compromised, resulting in increased nucleotide exchange and decreased GTP hydrolysis reactions (Bos, 1997; Drivas et al., 1990; Nakhaei-Rad et al., 2018). Mutations in this *RRAS2* hotspot region include p. Gly24_Gly26dup, p. Gly22_Gly24dup, p. Gly23Val, and p. Gly23Cys. Recent zebrafish model studies to test defective RAS signaling, whose genome also contains a *rras2* ortholog 98% similar to human. The embryos were cultured until three days after fertilization to measure the ceratohyal

angle, a mandibular structure which reflects the width and bluntness of the head, and measuring body length and relative head length (head length divided by body length). *RRAS2* in p. Gly24_Gly26dup leads to a significant increase in ceratohyal angle, a significant decrease in body length, and the observed increased incidence of pericardial effusion, which may highlight cardiac structural defects (Niihori et al., 2019). In our study, the five patients with Gly22 to Gly26 have been reported to have facial dysmorphism, broaden head circumference and prenatal features, with 2/5 having short stature, 3/5 intellectual disability, and 3/5 congenital heart disease.

Furthermore, Ala70 and Gln72 stabilize the switch I region by contacting Ile47 and Glu48, respectively, which are the binding sites for both *RRAS2* regulators (GEFs and GAPs) and effectors (Vetter & Wittinghofer, 2001). All pathogenic variants increase the activation of the

Patient 8	Patient 9	Patient 10	Patient 11	Patient 12	Patient 13	Patient 14	Patient 15
c.208G>A	c.208G>A	c.208G>A	c.70_78dup	c.70_78dup	c.65_73dup	c.68G>T	c.67G>T
p. Ala70Thr	p. Ala70Thr	p. Ala70Thr	p. Gly24_Gly-26dup	p. Gly24_Gly-26dup	p. Gly22_Gly-24dup	p. Gly23Val	p. Gly23Val
F	M	F	F	M	M	M	F
NA	–	Nuchal edema	NA	Polyhydramnios	Nuchal edema polyhydramnios	Polyhydramnios	Prenatal features
7years 1 month (–3.0 SD)	1 years 7 month (–1.8 SD)	8years 10 month (–2.1 SD)	6years (+0.2 SD)	18 month (+0.5 SD)	7 years 11 month (+0.3 SD)	12years 2 month (–1.5 SD)	9 years 2 month (–4.7 SD)
18 kg (–1.8 SD)	11 kg (–0.4 SD)	22kg (+1.9 SD)	NA	12.5kg (+0.7 SD)	27.5 kg (+0.5 SD)	32.5 kg (–1.4 SD)	18 kg (–3.1 SD)
52.5 cm (+0.4 SD)	49 cm (+0.2 SD)	52.5 cm (+0.2 SD)	NA	54 cm (+5.0 SD)	54 cm (+1.2 SD)	57 cm (+2.5 SD)	54.5 cm
Typical	Typical	Suggestive	Typical	Typical	Typical	Typical	Typical
Mild	–	–	NA	Mild	–	Mild	Mild
–	–	–	Macrocephaly	Enlarged ventricles	–	Chiari malformation	hydrocephalus
NA	NA	NA	Left	NA	NA	NA	Left
Bilateral ptosis	–	–	Mild myopia	Strabismic amblyopia, esotropia	–	Strabismus	–
–	–	VSD	Pulmonic stenosis	NA	Aortic stenosis	VSD	–
–	–	–	–	–	–	–	Embryonal rhabdomyosarcoma
–	–	Pectus excavatum	NA	–	–	–	–
Capri et al. (2019)	Capri et al. (2019)	Capri et al. (2019)	Niihori et al. (2019)	Capri et al. (2019)	Capri et al. (2019)	Capri et al. (2019)	

MAPK cascade and vary in impact cell morphology and cytoskeletal rearrangement. So far, it has been reported in the literature that in three patients with variants Ala70 and Gln72, all had ventriculomegaly, macrocephaly, and non-obstructive hydrocephalus detected by prenatal ultrasound at gestational age (Capri et al., 2019; Niihori et al., 2019; Weinstock & Sadler, 2022). Very few cases of NS accompanied by hydrocephalus have been reported (Fryns, 1997). Similarly, a Belgian group reported progressive hydrocephalus in up to 5% (3/62) of their NS patients (Fryns, 1997). In our study, the 10 patients with Ala70 and Gln72 exhibited typical facial dysmorphism, with 4/10 having neurology including macrocephaly, enlarged ventricles hydrocephalus, and delayed myelin development. In this study, our patient (P15) was found to have a heterozygous missense mutation of a pathogenic variant in the *RRAS2* gene (c.67G>T; p. Gly23Cys), located

in the pathogenic hotspot region or CCR region, and there were more than three deleterious mutations within 10 bp around the mutation. We observed that cranial MRI showed hydrocephalus, macrocephaly, and brain dysplasia from fetal life to 9 years of age.

All 15 patients showed forms suggestive of typical facial anomalies. Seven of them had mental disabilities ranging from mild to severe, and eight of them had heart abnormalities and ventricular septal defect (VSD), which were the most common anomalies of the heart in the reported literature, P3 was suspected tetralogy of Fallot (TOF), P15 was suspected fetal arrhythmia. Malignancy was reported in 13.3% (2/15) of the patients (P4, P15), and P4 died at the age of 9 weeks. 53.3% (8/15) neurological imaging found abnormalities, hydrocephalus (2/8), enlarged ventricles (2/8), Dandy-Walker variant (1/8), Chiari malformation (1/8), delayed myelin development

(1/8), only macrocephaly (1/8). 40% (6/15) eye abnormalities, and 20% (3/15) hearing loss. 20% (3/15) cryptorchidism, pectus excavatum was observed in P1, P2, and P10. Short stature was observed in 40% (6/15) of the patients (P1, P2, P5, P8, P10, P15). However, none of the patients was diagnosed with an abnormal kidney condition.

RRAS2 proteins containing amino acid substitutions analogous to those with an oncogenic role in *HRAS*, *KRAS*, and *NRAS* have transforming properties comparable to the strong transforming activity of RAS oncoproteins and similarly promote constitutive activation of the MAPK cascade. *RRAS2* controls multiple cellular processes, including proliferation, survival, and migration, and its functional dysregulation has been documented to contribute to oncogenesis, as well as activation of these mutations occurs in approximately 30% of human cancers (Bos, 1997; Cox & Der, 2010; Erdogan et al., 2007; Prior et al., 2012).

KRAS mutations were observed in ERMS that affected the genitourinary system, including the pelvis, paratesticular, vagina, and uterus. Three of these tumors showed regions of undifferentiated round cells and regions of spindle cell morphology, and the other three tumors showed primitive undifferentiated cells (Agaram et al., 2022). There is increasing evidence that Ras proteins have isoform-specific biological functions and tumorigenic effects, possibly attributed to the C-terminal hypervariable region and that different tumor types often display specificity in the involvement of the RAS gene, and different mutation codons could induce different transformation potentials (Prior et al., 2012). Indeed, many oncogenic variants of *RRAS2* have been reported, including the p. Gly23Val, p.-Ala70Thr, and p. Changes in Gln72Leu in a variety of solid tumors (Capri et al., 2019). The incidence and spectrum of benign and malignant tumors in NS and related diseases were reported in Kratz et al (Kashi et al., 2015). Recently, Kratz and colleagues reviewed the incidence of childhood cancer in 735 patients with germline mutations in the RAS-MAPK pathway gene, with two cases of rhabdomyosarcoma (RMS) observed in a cohort of a total of 12 cancer cases. Salem et al. reported that six total cases of RMS have been overall reported in NS, and three had a germline *SOS1* mutation. Three additional cases of embryonal rhabdomyosarcoma (ERMS) and NS (of the orbit, vagina, and abdomen) were reported, but genotype was not reported (Salem et al., 2016). Agaram et al. reported a homogeneous subset of ERMS with RAS mutations. Detection of 98 ERMS using MSK-IMPACT targeted DNA sequencing or Sanger sequencing revealed 54% *NRAS*, 23% *KRAS*, 19% *HRAS*, and 4% *BRAF*, and no *RRAS2* mutations (Agaram et al., 2022).

In this study, we found two cases with patients with malignancy, including a myeloproliferative disorder (P4) and one ERMS (P15). P15 with a heterozygous missense mutation in *RRAS2* who was diagnosed with abdominal cavity at 2 years of age, had tumor recurrence at 3 years of age after surgery, and had no recurrence of the tumor on follow-up after 1 year of whole abdominal radiotherapy. Our case of NS with ERMS caused by the *RRAS2* gene is quite rare. The ClinVar database for the *RRAS2* mutation site (c.67G>T) was reported in 2022, but the relevant data and the literature do not support it. Therefore, the clinical performance of our patient is considered quite important for the diagnosis of the NS 12 type, providing data support for the clinical diagnosis of the disease. The RAS/MEK/ERK pathway also plays an important role in rhabdomyosarcoma (RMS), as it can trigger uncontrollable proliferation of cancer cells and prolong their survival time. Mutations in RAS in zebrafish have been shown to lead to the development of ERMS (Kashi et al., 2015; Salem et al., 2016; Storer et al., 2013).

It is therefore generally accepted that there is a spectrum of activating mutations in the RAS-MAPK signaling pathway, in which germline mutations causing NS and other RASopathies tend to be less active, while somatic mutations causing cancer are more active. These findings broaden our understanding of the roles of *RRAS2* in human development, expanding the mutational landscape of NS and related disorders. More studies are needed to investigate the efficacy of these targeted drugs in patients with RAS-mutated RMS.

5 | CONCLUSIONS

On the whole, we reported the first NS patient with ERMS caused by *RRAS2* gene mutation in China, the clinical findings and genetic tests supported the diagnosis, but unfortunately, we were not able to complete functional assays of *RRAS2* variants. Our finding of the novel heterozygous *RRSA2* mutations expands the genetic causes of NS in the Chinese population. Additionally, the results from this study combined with those of other investigators implicate that RAS-MAPK molecular signaling lay a vital role in human neurodevelopmental and tumor. Once again, it is suggested that clinicians should consider NS and WES sequencing to help us diagnose when patients have symptoms such as stunted growth, heart disease, and tumor.

AUTHOR CONTRIBUTIONS

Lan Zeng and Shu-yao Zhu conceptualized the review; Lan Zeng and Shu-yao Zhu wrote the original draft; Lan

Zeng, Hui Zhu, Jin Wang and Yu Huang reviewed and edited the draft; Yi Deng, Ping Wei, Jing Nie, Bei Tang and Ai Chen explained the chromosome and WES results. All authors reviewed the article critically for intellectual content and agreed to the published version of the manuscript.

ACKNOWLEDGMENTS

We thank the families who participated in this study. We are grateful to the family for their willing participation and cooperation.

FUNDING INFORMATION

This research was funded by is supported by Chengdu Bureau of Science and Technology Project (2021-YF05-01658-SN).

CONFLICT OF INTEREST STATEMENT

The authors declare no conflict of interest.

DATA AVAILABILITY STATEMENT

Suggested Data Availability Statements are available in section ClinVar bank at [VCF001342092.3-ClinVar-NCBI \(nih.gov\)](https://www.ncbi.nlm.nih.gov/clinvar/study/VCF001342092.3).

ETHICS STATEMENT

The study was conducted in accordance with the Declaration of Helsinki, and approved by the Institutional Ethics Statement of Sichuan Provincial Maternity and Child Health Care Hospital (Protocol 20230331-027 and date of 2023.03.31).

INFORMED CONSENT STATEMENT

Informed consent was obtained from all subjects involved in the study. Written informed consent has been obtained from the patient(s) to publish this paper if applicable.

ORCID

Shuyao Zhu  <https://orcid.org/0000-0003-2169-8340>

REFERENCES

- Agaram, N. P., Huang, S. C., Tap, W. D., Wexler, L. H., & Antonescu, C. R. (2022). Clinicopathologic and survival correlates of embryonal rhabdomyosarcoma driven by RAS/RAF mutations. *Genes, Chromosomes & Cancer*, *61*(3), 131–137.
- Bos, J. L. (1997). Ras-like GTPases. *Biochimica et Biophysica Acta*, *1333*(2), M19–M31.
- Capri, Y., Flex, E., Krumbach, O. H. F., Carpentieri, G., Cecchetti, S., Lissewski, C., Rezaei Adariani, S., Schanze, D., Brinkmann, J., Piard, J., Pantaleoni, F., Lepri, F. R., Goh, E. S., Chong, K., Stieglitz, E., Meyer, J., Kuechler, A., Bramswig, N. C., Sacharow, S., ... Zenker, M. (2019). Activating mutations of RRAS2 are a rare cause of Noonan syndrome. *American Journal of Human Genetics*, *104*(6), 1223–1232.
- Cox, A. D., & Der, C. J. (2010). Ras history: The saga continues. *Small GTPases*, *1*(1), 2–27.
- Drivas, G. T., Shih, A., Coutavas, E., Rush, M. G., & D'Eustachio, P. (1990). Characterization of four novel ras-like genes expressed in a human teratocarcinoma cell line. *Molecular and Cellular Biology*, *10*(4), 1793–1798.
- Erdogan, M., Pozzi, A., Bhowmick, N., Moses, H. L., & Zent, R. (2007). Signaling pathways regulating TC21-induced tumorigenesis. *The Journal of Biological Chemistry*, *282*(38), 27713–27720.
- Fryns, J. P. (1997). Progressive hydrocephalus in Noonan syndrome. *Clinical Dysmorphology*, *6*(4), 379.
- Graham, S. M., Oldham, S. M., Martin, C. B., Drugan, J. K., Zohn, I. E., Campbell, S., & Der, C. J. (1999). TC21 and Ras share indistinguishable transforming and differentiating activities. *Oncogene*, *18*(12), 2107–2116.
- Kashi, V. P., Hatley, M. E., & Galindo, R. L. (2015). Probing for a deeper understanding of rhabdomyosarcoma: Insights from complementary model systems. *Nature Reviews. Cancer*, *15*(7), 426–439.
- Nakhaei-Rad, S., Haghighi, F., Nouri, P., Rezaei Adariani, S., Lissy, J., Kazemineh, N. S., Dvorsky, R., & Ahmadian, M. R. (2018). Structural fingerprints, interactions, and signaling networks of RAS family proteins beyond RAS isoforms. *Critical Reviews in Biochemistry and Molecular Biology*, *53*(2), 130–156.
- Niihori, T., Nagai, K., Fujita, A., Ohashi, H., Okamoto, N., Okada, S., Harada, A., Kihara, H., Arbogast, T., Funayama, R., Shirota, M., Nakayama, K., Abe, T., Inoue, S. I., Tsai, I. C., Matsumoto, N., Davis, E. E., Katsanis, N., & Aoki, Y. (2019). Germline-activating RRAS2 mutations cause Noonan syndrome. *American Journal of Human Genetics*, *104*(6), 1233–1240.
- Prior, I. A., Lewis, P. D., & Mattos, C. (2012). A comprehensive survey of Ras mutations in cancer. *Cancer Research*, *72*(10), 2457–2467.
- Roberts, A. E., Allanson, J. E., Tartaglia, M., & Gelb, B. D. (2013). Noonan syndrome. *The Lancet*, *381*(9863), 333–342.
- Salem, B., Hofherr, S., Turner, J., Doros, L., & Smpokou, P. (2016). Childhood rhabdomyosarcoma in association with a RASopathy clinical phenotype and mosaic germline SOS1 duplication. *Journal of Pediatric Hematology/Oncology*, *38*(8), e278–e282.
- Storer, N. Y., White, R. M., Uong, A., Price, E., Nielsen, G. P., Langenau, D. M., & Zon, L. I. (2013). Zebrafish rhabdomyosarcoma reflects the developmental stage of oncogene expression during myogenesis. *Development*, *140*(14), 3040–3050.
- Tartaglia, M., Gelb, B. D., & Zenker, M. (2011). Noonan syndrome and clinically related disorders. *Best Practice & Research. Clinical Endocrinology & Metabolism*, *25*(1), 161–179.
- Tidyman, W. E., & Rauen, K. A. (2009). The RASopathies: Developmental syndromes of Ras/MAPK pathway dysregulation. *Current Opinion in Genetics & Development*, *19*(3), 230–236.
- Vetter, I. R., & Wittinghofer, A. (2001). The guanine nucleotide-binding switch in three dimensions. *Science*, *294*(5545), 1299–1304.
- Weinstock, N. I., & Sadler, L. (2022). The RRAS2 pathogenic variant p.Q72L produces severe Noonan syndrome with hydrocephalus: A case report. *American Journal of Medical Genetics. Part A*, *188*(1), 364–368.

- Yamamoto, G. L., Agüena, M., Gos, M., Hung, C., Pilch, J., Fahiminiya, S., Abramowicz, A., Cristian, I., Buscarilli, M., Naslavsky, M. S., Malaquias, A. C., Zatz, M., Bodamer, O., Majewski, J., Jorge, A. A. L., Pereira, A. C., Kim, C. A., Passos-Bueno, M. R., & Bertola, D. R. (2015). Rare variants in *SOS2* and *LZTR1* are associated with Noonan syndrome. *Journal of Medical Genetics*, 52(6), 413–421.
- Yu, C., Lyn, N., Li, D., Mei, S., Liu, L., & Shang, Q. (2023). Clinical analysis of Noonan syndrome caused by *RRAS2* mutations and literature review. *European Journal of Medical Genetics*, 66(1), 104675.

How to cite this article: Zeng, L., Wang, J., Zhu, H., Huang, Y., Deng, Y., Wei, P., Nie, J., Tang, B., Chen, A., & Zhu, S. (2024). The *RRAS2* pathogenic variant (c.67G>T; p. Gly23Cys) produces Noonan syndrome with embryonal rhabdomyosarcoma. *Molecular Genetics & Genomic Medicine*, 12, e2313. <https://doi.org/10.1002/mgg3.2313>